

## Solid-State $^1\text{H}$ and $^{29}\text{Si}$ NMR Studies of Silicate and Borosilicate Gel to Glass Conversion

Kyung Hwa Yang and Ae Ja Woo\*

Department of Chemistry, Ewha Womans University, Seoul 120-750, Korea

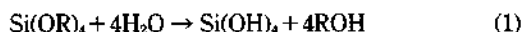
\*Department of Science Education, Ewha Womans University, Seoul 120-750, Korea

Received February 27, 1996

Silicate and borosilicate gels were prepared by the sol-gel process and thermally treated in the 150-850 °C temperature range. Solid-state  $^1\text{H}$  MAS and  $^{29}\text{Si}$  CP/MAS NMR spectroscopy were used to investigate the effects of heat treatments on the silicate gel to glass conversion process. The  $^1\text{H}$  NMR isotropic chemical shifts and the relative intensities of hydrogen bonded and isolated silanol groups have been used to access the information concerning the dehydration process on the silicate gel surface. The  $^{29}\text{Si}$  NMR isotropic chemical shifts affected by the local silicon environment have been used to determine the degree of crosslinking, *i.e.* the number of siloxane bonds. These NMR results suggest that the silicate gel to glass conversion process is occurred by two stages which are dependent on the temperature; (1) the formation of particles up to 450 °C and (2) the formation of large particles by aggregation of each separated single particle above 450 °C. In addition, the effects of B atom on the formation of borosiloxane bonds in borosilicates have been discussed.

### Introduction

Recently, the sol-gel process<sup>1-3</sup> instead of conventional melting process has become an increasingly important method for the preparation of the ceramics and glasses because of many advantages such as better homogeneity and purity, lower temperature of preparation, etc. The sol-gel process is characterized by a step-growth polymerization composed of two reactions, hydrolysis and condensation, described by Eqs. (1) and (2).



The local silicon environment is described as  $Q^n$  ( $n=0,1,2,3,4$ ) nomenclature,<sup>4</sup>  $-\text{Si}(\text{O}-\text{Si})_n$ , which represents the extent of crosslinking. The basic component of glasses is silicon dioxide ( $\text{SiO}_2$ ). The multicomponent metal oxides prepared by adding metal oxides such as  $\text{Al}_2\text{O}_3$ ,  $\text{Na}_2\text{O}_3$ ,  $\text{B}_2\text{O}_3$ ,  $\text{Li}_2\text{O}_3$ ,  $\text{Fe}_2\text{O}_3$ ,  $\text{TiO}_2$ , etc. to  $\text{SiO}_2$  give the glasses of the different structures and properties. One of the most popular multicomponent metal oxides is borosilicate ( $\text{SiO}_2\text{-B}_2\text{O}_3$ ) characterized by the borosiloxane bond ( $\equiv\text{Si}-\text{O}-\text{B}=\text{O}$ ), which shows the properties of lower thermal expansion coefficient, high dielectric constant, and good chemical resistance.<sup>2</sup>

Solid-state multinuclear NMR spectroscopy has been used to study the structures and dynamics of sol-gel materials.  $^1\text{H}$  MAS and CRAMPS NMR techniques have been used to characterize the bonding state of the hydrous species.<sup>5-7</sup>  $^{11}\text{B}$  MAS<sup>8,9</sup> and DAS<sup>10</sup> NMR have been applied to detect multiple boron sites from the  $^{11}\text{B}$  isotropic chemical shifts and quadrupole parameters.  $^{17}\text{O}$  NMR spectroscopy has provided information about the hydrolysis and condensation reactions.<sup>11</sup>  $^{29}\text{Si}$  CP/MAS NMR technique has been used to detect the  $Q^n$  local silicon sites from the  $^{29}\text{Si}$  isotropic chemical shifts for the determination of the extent of completion of the hydro-

lysis and condensation reaction which is contributed to the structural evolution.<sup>12</sup> In addition, dynamic information on the exchange of  $Q^n$  silicon sites was obtained from the lineshape analyses and  $T_1$  measurements.<sup>13</sup>

In this work we are trying to investigate the structural evolution during the silicate gel to glass conversion by using solid-state  $^1\text{H}$  and  $^{29}\text{Si}$  NMR spectroscopy. The principal objectives are as follows: (1) how does the silanol group ( $\equiv\text{Si}-\text{OH}$ ) on the silicate gel surface change during the gel to glass conversion and what does it affect on the formation of siloxane bond ( $\equiv\text{Si}-\text{O}-\text{Si}=\text{O}$ )? (2) What is the function of B atoms in the formation of borosiloxane bond ( $\equiv\text{Si}-\text{O}-\text{B}=\text{O}$ ) in borosilicate gel?

### Experimental

**Sample Preparation.** All chemicals were purchased from Aldrich Chemical Company, Inc. Table 1 describes the details of sample preparation based on the four steps of sol-gel process; mixing, aging, drying, and stabilization. The molar compositions of silicate and borosilicate solutions are  $\text{TEOS}(\text{Si}(\text{OEt})_4)/\text{H}_2\text{O}/\text{EtOH}=1.0/5.0/8.5$  and  $\text{TEOS}(\text{Si}(\text{OEt})_4)/(\text{H}_2\text{O})_x/\text{EtOH}/\text{B}(\text{OEt})_3=0.85/4.25/0.75/8.50/0.15$ , respectively. In order to prepare the homogeneous borosilicate gel, slowly hydrolyzed TEOS relative to  $\text{B}(\text{OEt})_3$  and  $(\text{H}_2\text{O})_x$  were mixed firstly and then  $\text{B}(\text{OEt})_3$  and  $(\text{H}_2\text{O})_x$  were mixed to form the crosslinking. After drying step, borosilicate gels containing above 40% boron show the second phase consisted of the nontransparent white powder analyzed as boric acid.<sup>14</sup> Sample labels based on the stabilization temperature are denoted on Table 1.

**Solid-State  $^1\text{H}$  and  $^{29}\text{Si}$  NMR Spectroscopy.**  $^1\text{H}$  MAS and  $^{29}\text{Si}$  CP/MAS NMR spectra were obtained on a Bruker MSL200 solid-state NMR spectrometer operating at 200 MHz and 39.7 MHz, respectively, using a 5 kHz CP/MAS probe and a 7 mm  $\text{ZrO}_2$  rotor with a Kel-F cap. The MAS (Magic Angle Spinning) was performed at  $\sim 3.5$  kHz and

\*To whom correspondence should be addressed.

**Tables 1.** Sample Preparation Procedure by Sol-Gel Process

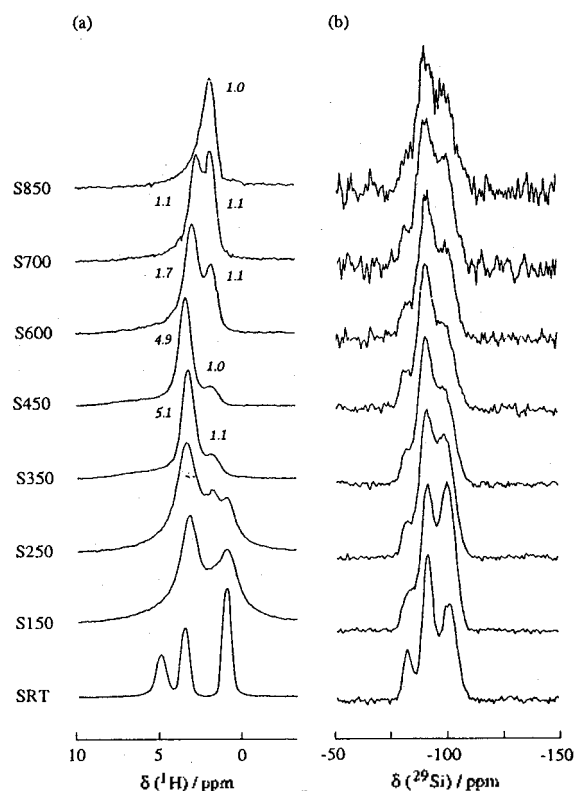
Sol-Gel Process Step	Silicate	Borosilicate
Mixing	TEOS+EtOH+H <sub>2</sub> O	TEOS+EtOH+(H <sub>2</sub> O) <sub>2</sub>
	↓	↓
	stir, 2 hrs, room temp.	stir, 26 hrs, room temp.
Aging	↓	↓
		B(OEt) <sub>3</sub> +(H <sub>2</sub> O) <sub>2</sub>
		stir, 2 hrs, room temp.
Drying	2 days, 50 °C	2 days, 60 °C
	↓	↓
Stabilization	4 days, 50 °C	4 days, 70 °C
	↓	↓
	Heat Treatment	Heat Treatment
	room temp.-SRT*	150 °C - BS150*
	150 °C - S150	450 °C - BS450
	250 °C - S250	700 °C - BS700
	350 °C - S350	
	450 °C - S450	
600 °C - S600		
700 °C - S700		
850 °C - S850		

\*Sample Labels

CP (Cross Polarization) technique *via* proton was used to enhance the signal-to-noise ratio. The <sup>1</sup>H MAS spectra were acquired as simple Bloch decays. Natural abundance <sup>29</sup>Si CP/MAS spectra were taken *via* a standard single contact Hartmann Hahn Cross Polarization pulse sequence. The <sup>1</sup>H 90° pulse length was 4 μs and the recycle time was 10 s. The cross polarization contact time was 20 ms, which was experimentally adjusted to obtain the maximum signal-to-noise ratio. The <sup>1</sup>H and <sup>29</sup>Si chemical shift values recorded on the δ-scale are referenced through external tetrakis(trimethyl)silane (TTMS) to TMS.

## Results and Discussion

**<sup>1</sup>H and <sup>29</sup>Si NMR of Silicate.** Figures 1(a) and (b) show the solid-state <sup>1</sup>H MAS and <sup>29</sup>Si CP/MAS spectra of silicates, respectively, treated at various stabilization temperatures. The <sup>1</sup>H MAS spectrum of SRT sample shows three peaks. Two peaks at 1.1 and 3.7 ppm are assigned to -CH<sub>3</sub> and -CH<sub>2</sub> groups of ethanol based on the <sup>1</sup>H isotropic chemical shifts and their relative intensities. Another peak at 6.3 ppm corresponds to -OH groups from ethanol and molecular water. This broad peak may be due to the fast <sup>1</sup>H exchange between -OH groups. Even though the <sup>29</sup>Si CP/MAS spectrum of SRT represents the formation of a large number of Q<sup>2</sup> (-83 ppm), Q<sup>3</sup> (-93 ppm), and Q<sup>4</sup> (-101 ppm) local silicon sites, the <sup>1</sup>H MAS peak acquired from the silanol groups (≡Si-OH) is not observed because of the relatively low concentration. The big difference between the <sup>1</sup>H MAS



**Figures 1.** Solid-state (a) <sup>1</sup>H MAS and (b) <sup>29</sup>Si CP/MAS NMR spectra for silicates treated at various stabilization temperatures. Experimental parameters are as follows (NS=number of scans, RD=relaxation delay): NS=12 (<sup>1</sup>H MAS) and 200 (<sup>29</sup>Si CP/MAS), RD=10 s. The numbers on the <sup>1</sup>H MAS spectra normalized to the peak intensity of *i*-OH group of S850 refer to the absolute <sup>1</sup>H peak intensities of *h*-OH and *i*-OH groups. Because S150 and S250 spectra still represent the ethanol and water peaks, they are excluded from the comparison of the absolute peak intensities.

spectra obtained from SRT and S150 samples is caused by the evaporation of molecular water (physisorbed water) and ethanol. On the heat treatment at 150 °C, we measured about 50% loss in weight of S150 compared with SRT. In addition, the increase of Q<sup>4</sup> peak intensity in <sup>29</sup>Si CP/MAS spectrum of S150 relative to SRT indicates that heat treatment above 150 °C causes the rate of condensation reaction rapid.

Figure 2 shows the nonlinear least-squares analysis to the <sup>1</sup>H MAS spectrum of S250. Lorentzian function has been used to calculate the peak shapes and intensities. The best fit to the experimental spectrum is composed of five components; molecular water (5.5 ppm), -CH<sub>2</sub> (3.7 ppm) and -CH<sub>3</sub> (1.1 ppm) groups from ethanol, and hydrogen bonded ≡Si-OH (*h*-OH, 3.5 ppm) and isolated ≡Si-OH (*i*-OH, 2.0 ppm) groups on the silicate gel surface. From the result shown in Figure 2 that the relative <sup>1</sup>H peak intensity of the *h*-OH group is about 4 times bigger than that of the *i*-OH group, we can expect there exist a lot of hydrogen bonds between the ≡Si-OH groups on the silicate gel surface.

In the 150-450 °C temperature range, based on the absolute <sup>1</sup>H peak intensities represented in Figure 1(a), we have observed that the *h*-OH groups decrease while the *i*-OH groups

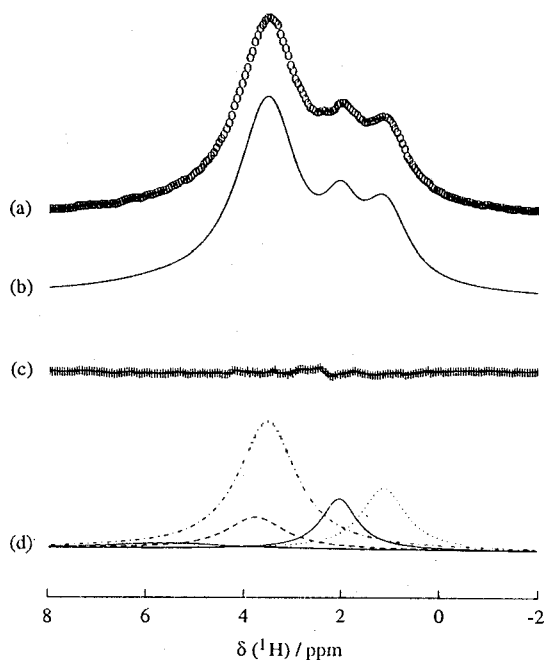


**Figure 2.** Solid-state  $^1\text{H}$  MAS NMR spectrum for S250 sample and the corresponding nonlinear least-squares fit. (a) experimental  $^1\text{H}$  MAS spectrum, (b) best calculated fit to the experimental spectrum, and (c) the corresponding residuals. The fit calculated from Lorentzian function is composed of five components as shown in (d). The five components are molecular water (—),  $-\text{CH}_2$  (---) and  $-\text{CH}_3$  (···) from ethanol,  $h\text{-OH}$  (-·-·), and  $i\text{-OH}$  (—). The calculated ratio of the peak intensities of molecular water/ $-\text{CH}_2$ / $-\text{CH}_3$ / $h\text{-OH}$ / $i\text{-OH}$  is 3.0/1.0/23.3/6.0.

increase. This leads to the conclusions that the dehydration process is occurred by elimination of chemisorbed water between  $h\text{-OH}$  groups and consequently the formation of  $i\text{-OH}$  groups, which contributes to the formation of harder particles than the flexible SRT sample. This fact also can be supported by the  $^{29}\text{Si}$  CP/MAS spectra. Decrease of the relative  $\text{Q}^4$  peak intensity implies that the changes in the rate of polarization transfer *via* proton may be caused by the decreased number of protons nearby  $\text{Q}^4$  silicon sites.

On the heat treatment above  $450^\circ\text{C}$ , we have observed the followings from the  $^1\text{H}$  MAS spectra: (1) both  $h\text{-OH}$  and  $i\text{-OH}$  peak intensities still change and finally only  $i\text{-OH}$  peak remains for S850 sample; the  $h\text{-OH}$  groups decrease while the  $i\text{-OH}$  groups are constant. (2) the  $^1\text{H}$  isotropic chemical shifts for  $h\text{-OH}$  peaks from S450 to S700 samples shift to  $\sim 0.8$  ppm lower frequency (upfield shift). According to the experimental and theoretical studies about the dependence of the  $^1\text{H}$  isotropic chemical shifts on the hydrogen bonding strength,<sup>15–18</sup> the result indicates that the hydrogen bonding strength between Si-OH groups becomes weaker with increasing stabilization temperature. That is, the distance between the Si-OH groups on the silicate gel surface becomes farther and at  $850^\circ\text{C}$  the distance is longer than van der Waals distance ( $\sim 330$  pm). From two observations, it is evident that the dehydration process is occurred *via* elimination of chemisorbed water between the  $h\text{-OH}$  groups on the adjacent gel surface, in which large particles by the aggregation

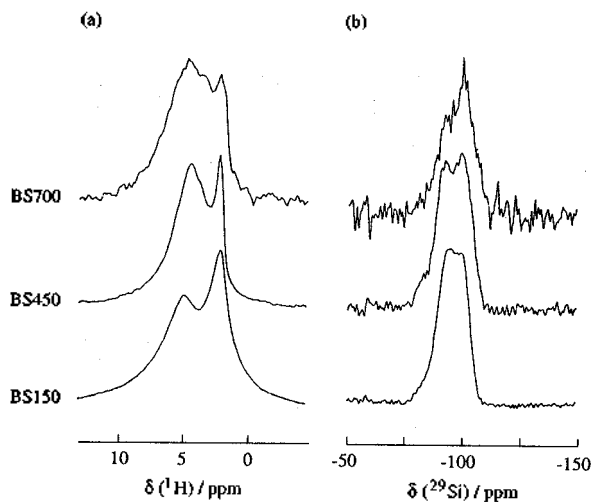
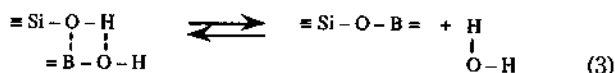


**Figure 3.** Solid-state (a)  $^1\text{H}$  MAS and (b)  $^{29}\text{Si}$  CP/MAS NMR spectra for borosilicates treated at various stabilization temperatures. Experimental parameters are as follows: NS=4~8 ( $^1\text{H}$  MAS) and 120~240 ( $^{29}\text{Si}$  CP/MAS), RD=10 s.

of each separated single particle are formed. Almost constant ratio of  $\text{Q}^2/\text{Q}^3/\text{Q}^4$  peak intensities as shown in the  $^{29}\text{Si}$  CP/MAS spectra suggests that only a small number of  $\text{Q}^2$  or  $\text{Q}^3$  local silicon sites are necessary for the formation of  $\text{Q}^4$  sites, which also provides the information about the dehydration process as mentioned above. These NMR results are consistent with the Raman studies.<sup>19,20</sup> The nonequilibrium aggregation of each separated single particle can be modeled by using fractal concepts<sup>21</sup> to investigate the fractal dimension and the kinetics. The diffusion-limited aggregation (DLA) model introduced by Witten-Sander<sup>22,23</sup> and the Monte Carlo method on two-dimensional square lattices have been used for the simulations.

**$^1\text{H}$  and  $^{29}\text{Si}$  NMR of Borosilicate.** Figures 3(a) and (b) show the solid-state  $^1\text{H}$  MAS and  $^{29}\text{Si}$  CP/MAS spectra of borosilicates, respectively, treated at various stabilization temperatures. On comparing the absolute  $^1\text{H}$  peak intensities of borosilicates with those of silicates, we have found that the  $i\text{-OH}$  groups in borosilicates are independent on the stabilization temperature. Large  $i\text{-OH}$  peak intensities of spectra especially mean that the condensation reaction in borosilicates is occurred by the crosslinks between Si and B atoms, and the  $\equiv\text{Si-O-B}=\text{O-H}$  bonds are formed through the reaction described by Eq. (3).<sup>14</sup>



However, because the reverse reaction can be dominated by hydrolysis with remaining molecular water,<sup>9</sup> it is possible to form the borosilicate network by the heat treatment above  $150^\circ\text{C}$ . This fact is supported by the study that the  $\equiv\text{Si-O-B}=\text{O}$  bonds are not found in incompletely dried borosilicate gels.<sup>24</sup>

Figure 3(a) shows that the  $h\text{-OH}$  peak widths of the borosilicates are much broader than those of silicates, while the  $i\text{-OH}$  peak widths have no change. Based on the study about

the  $^1\text{H}$  isotropic chemical shift values of Si-OH and B-OH groups by Fleischer *et al.* study,<sup>25</sup> we can expect that the broader *h*-OH peaks must be composed of three kinds of protons; 4-coordinated Si-OH (tetrahedral  $\text{SiO}_2$ ) and 3-/4-coordinated B-OH (trigonal  $\text{BO}_3$ /tetrahedral  $\text{BO}_4$ ).<sup>8</sup> Because there is no difference in the  $^1\text{H}$  peak widths obtained from Si-OH, B-OH, and Al-OH groups,<sup>24</sup> the linebroadening caused by the quadrupole interaction with  $^{11}\text{B}$  nuclei can be neglected. In addition, the unchanged *i*-OH peak widths suggest that most of the *i*-OH peak intensities are acquired from the Si-OH groups. The oxophilicity of B atoms in  $\text{BO}_3$  and lower B-O bond energy in  $\text{BO}_4$  lead to accept the electrons for the formation of  $\text{BO}_4$ . Thus, if there exist some remaining solvent and molecular water, B atom is more accessible to O atom for the formation of tetrahedral environment. The effects of heat treatments on the local boron sites,  $\text{BO}_3$  or  $\text{BO}_4$ , in borosilicates are now studied in our laboratory by using solid-state  $^{11}\text{B}$  nutation NMR spectroscopy.

Figure 3(b) shows that the  $\text{Q}^4$  peak intensities relative to  $\text{Q}^2$  and  $\text{Q}^3$  in borosilicates are bigger than those in silicates. The reason can be that boron alkoxide is rapidly hydrolyzed and existed as boric acid. The measured pHs for silicate and borosilicate solutions are 4.8 and 4.0, respectively. Such a more acidic condition makes the condensation reaction more fast,<sup>11</sup> therefore the number of  $\text{Q}^4$  sites are increased.

### Conclusions

The structural conversion of silicate gel to glass has been investigated in 150-850  $^\circ\text{C}$  temperature range by using solid-state  $^1\text{H}$  and  $^{29}\text{Si}$  NMR spectroscopy. It has been confirmed that the conversion process is continuous and dependent on the stabilization temperature as follows: (1) Most solvent and molecular water are evaporated below 150  $^\circ\text{C}$ . (2) In the 150-450  $^\circ\text{C}$  temperature range, the dehydration on the flexible silicate gel surface leads to the solid particles. (3) Above 450  $^\circ\text{C}$ , the dehydration by the aggregation of each separated particle produces more condensed and larger particles. (4) The silicate gel to glass conversion process is completed at 850  $^\circ\text{C}$ .

The incorporation of boron in silicate backbone provides the formation of  $\equiv\text{Si-O-B}=\text{}$  bonds which characterize the properties and structures of borosilicate gels. The  $\equiv\text{Si-O-B}=\text{}$  bonds are kept by the heat treatment above 150  $^\circ\text{C}$ .

**Acknowledgment.** This work was supported by Faculty Research Grant (1994) funded by Ewha Womans University. Korea Basic Science Center is acknowledged for the use of the Bruker MSL200 NMR spectrometer.

### References

- Hench, L. L.; West, J. K. *Chem. Rev.* **1990**, *90*, 33.
- Brinker, C. J.; Scherer, G. W. *Sol-Gel Science*; Academic Press: San Diego, 1990.
- Hoang, G. C. Ph.D. Thesis, Texas Christian University, 1989.
- Engelhardt, G.; Jancke, H.; Hoebbel, D.; Wolfgang, W. *Z. Chem.* **1974**, *14*, 109.
- Bray, P. J.; Holupka, E. J. *J. Non-Crystalline Solids* **1984**, *67*, 119.
- Bronnimann, C. E.; Zeigler, R. C.; Maciel, G. E. *J. Am. Chem. Soc.* **1988**, *110*, 2023.
- Eckert, H.; Yesinowski, J. P.; Silver, L. A.; Stolper, E. M. *J. Phys. Chem.* **1988**, *92*, 2055.
- Turner, G. L.; Smith, K. A.; Kirkpatrick, R. J.; Oldfield, E. J. *Magn. Reson.* **1986**, *67*, 544.
- Irwin, A. D.; Holmgren, J. S.; Jonas, J. *J. Non-Crystalline Solids* **1988**, *101*, 249.
- Youngman, R. E.; Zwanziger, J. W. *J. Non-Crystalline Solids* **1994**, *168*, 293.
- Turner, C. W.; Franklin, K. J. *J. Non-Crystalline Solids* **1987**, *91*, 402.
- Vega, A. J.; Scherer, G. W. *J. Non-Crystalline Solids* **1989**, *111*, 153.
- Stebbins, J. F. *J. Non-Crystalline Solids* **1988**, *106*, 359.
- Irwin, A. D.; Holmgren, J. S.; Zerda, T. W.; Jonas, J. *J. Non-Crystalline Solids* **1987**, *89*, 191.
- Fukui, H.; Miura, K.; Yamazaki, H.; Nosaka, T. *J. Chem. Phys.* **1985**, *82*, 1410.
- Ratcliffe, C. I.; Ripmeester, J. A.; Tse, J. S. *Chem. Phys. Letters* **1985**, *120*, 427.
- Yesinowski, J. P.; Eckert, H. *J. Am. Chem. Soc.* **1987**, *109*, 6274.
- White, J. L.; Beck, L. W.; Haw, J. F. *J. Am. Chem. Soc.* **1992**, *114*, 6182.
- Krol, D. M.; van Lierop, J. G. *J. Non-Crystalline Solids* **1984**, *63*, 131.
- Rousset, J. L.; Duval, E.; Boukenter, A.; Champagnon, B.; Monteil, A. *J. Non-Crystalline Solids* **1988**, *107*, 27.
- Mandelbrot, B. B. *The Fractal Geometry of Nature*; Freeman: San Francisco, 1982.
- Witten, T. A.; Sander, L. M. *Phys. Rev. Lett.* **1981**, *47*, 1400.
- Witten, T. A.; Sander, L. M. *Phys. Rev. B* **1983**, *27*, 5686.
- Mukherjee, S. P. *J. Non-Crystalline Solids* **1984**, *63*, 35.
- Fleischer, U.; Kutzelnigg, W.; Bleiber, A.; Sauer, J. *J. Am. Chem. Soc.* **1993**, *115*, 7833.